Dicle Üniversitesi Veteriner Fakültesi Dergisi
Dicle University Journal of Faculty of Veterinary Medicine

e-ISSN:1308-0679
https://dergipark.org.tr/tr/pub/duvetfd

DERLEME
REVIEW

3D Modeling and Printing Technology in Veterinary Anatomy

Gülseren KIRBAŞ DOĞAN[1,a,✉], Evin KAÇMAZ[1,b]

[1]Department of Anatomy, Faculty of Veterinary Medicine, University of Kafkas, Kars, TÜRKİYE

ORCID: [a]0000-0003-3770-9956, [b]0009-0009-0920-9066

✉ Sorumlu Yazar

Gülseren KIRBAŞ DOĞAN
Department of Anatomy, Faculty of Veterinary Medicine, University of Kafkas, Kars, TÜRKİYE

glsrn36@gmail.com

Received
14.07.2025

Accepted
10.10.2025

Published
31.12.2025

DOI

10.47027/duvetfd.1741889

How to cite: **Kırbaş Doğan G, Kaçmaz E (2025).** 3D modeling and printing technology in veterinary anatomy. *Dicle Univ Vet Fak Derg*., 18(2):193-204.

Abstract

Anatomy examines the structure of living things, the organs within them, and the functioning of these organs within certain systems. Various materials are used when looking at these anatomic structures. Even though organs placed in formaldehyde, liquid foam soap, ethanol, and citric acid are kept from decaying for a long time, inhaling this liquids or coming into direct contact with it poses a health risk. Today, the advancement of technology and its use in almost all areas has been reflected in veterinary anatomy field. Anatomical structures can be examined in 3D using imaging methods and various software. This allows us to examine anatomical structures that are difficult to access and small-sized anatomical formations. Materials can be obtained from these models using various 3D printing devices. This makes it possible to work in more hygienic conditions with less contamination with harmful chemicals such as formaldehyde. The presented study systematically compiles scientific research related to 3D modeling and printing technology in the field of veterinary anatomy. An attempt was made to explain the current state of 3D in veterinary anatomy through systematically compiled studies on the basis of animal species. It is expected to serve as a guide for future studies in this area.

Key Words: Anatomy, 3d modeling, systems, technology, veterinary

Veteriner Anatomide 3B Modelleme ve Baskı Teknolojisi

Öz

Anatomi canlının yapısını, içinde yer alan organları ve bu organların belirli sistemler dahilinde çalışmasını inceler. Bu anatomik yapılar anlatılırken çeşitli materyaller kullanılır. Formaldehit, sıvı köpük sabun, etanol ve sitrik asit çözeltisi içerisine konan organlar uzun süre çürümeden tutulsa da bu sıvıların solunması, birebir temasta bulunulması sağlığı tehdit etmektedir. Günümüzde teknolojinin de ilerlemesi ve neredeyse tüm alanlarda kullanımı veteriner anatomi alanına da yansımıştır. Görüntüleme yöntemleri ve çeşitli yazılımlar kullanılarak anatomik yapılar 3B olarak incelenebilir. Böylelikle erişimi zor olan anatomik yapılar ve küçük boyutlardaki anatomik oluşumlara bakalabilme imkanı sunulmaktadır. Çeşitli 3B baskı cihazları kullanılarak bu modellerden materyaller elde edilebilmektedir. Böylelikle formaldehit gibi zararlı kimyasallarla daha az kontaminasyonla daha hijyenik koşullarda çalışmak mümkündür. Sunulan çalışmada veteriner anatomi alanında 3B modelleme ve baskı teknolojisiyle alakalı bilimsel çalışmalar sistemsel olarak biraraya getirildi. Hayvan türü bazında sistemsel olarak derlenen çalışmalarla 3B'nin veteriner anatomide geldiği nokta anlatılmaya çalışıldı. Bu konuda yapılacak olan çalışmalara yol gösterici olacağı düşünülmektedir.

Anahtar Kelimeler: Anatomi, 3B modelleme, sistemler, teknoloji, veteriner

INTRODUCTION

Veterinary anatomy is one of the cornerstones of veterinary medicine. This course uses various materials (1). Although dissection allows three-dimensional examination of anatomical structures, this method leads to the death of many animals. In addition, the harmful effects of formaldehyde and the challenges of examining small structures are significant issues (2). Today, various technological tools and platforms are used to support educational activities. These include 3D modeling and printing technology (3). 3D imaging and augmented reality applications are becoming increasingly common. These methods enable clearer visualisation of hard-to-reach areas, spatial depth monitoring from different angles, and access to learning materials at any time (4,5). Data obtained from tissues and/or organs can be converted into 3D models using various imaging techniques. This process is called reconstruction or reformation. This method facilitates an understanding of irregular surfaces and enables various changes to be made to them (6,7). Studies have shown that physical materials taken from 3D models help students to understand and study anatomical structures more effectively (8).

Imaging methods are used as a term that encompasses all diagnostic methodologies used to create a visual representation of body structures. 3D reconstruction of various structures can be done using imaging techniques (6). These include computed tomography (CT), magnetic resonance imaging (MRI), conventional radiography, ultrasound, and nuclear medicine. CT, MRI, radiography, and ultrasound are the most commonly used non-invasive imaging methods in veterinary medicine. CT is based on the principle that differences in the absorption of X-rays become visible (9). CT, which has a place in the field of veterinary medicine in the diagnosis of neurological, oncological, and orthopedic diseases, was applied in the diagnosis of neoplasm cases in dogs in 1980-1981 (10,11). It is an imaging technique for obtaining images by taking sections from the body (12). The most important advantages of CT are that it can be used effectively in structures containing voids and that it can provide a high level of detail in cross-sectional images (11,13). In MRI, a signal is produced as a result of the interaction of protons in the tissues with a strong magnetic field and radiofrequency pulses. The contrast in the resulting magnetic resonance (MR) image reflects the water content of different tissues. It is generally used in soft tissues (9). This method, discovered in the 1940s, began to be implemented only in the 1970s and 1980s. MRI is also used in pet animals in diagnosis and diagnostic processes (11,14). Biological images obtained from CT and MRI are exported as cross-sectional images in a standard data format called Digital Imaging and Communications Format in Medicine (DICOM). DICOM images are used to create 3D models (15). Structures can be obtained from these images with 3D printing technology (16).

One of the most common methods used for 3D printing is 3D scanning. It's particularly popular for creating and printing digital versions of hard tissues and organs. 3D printing technology is based on engineering. The aim here is to create a prototype for a structure or to produce a part. While it was a time-consuming and expensive process at first, there was a tendency towards methods that took less time and money. This continued to gain momentum in the 1980s. Later, computer-aided drawing (CAD) was produced (16). The 3D printer was invented by Chuck Hull in 1986 (17). In 3D printing, a layered manufacturing process is used to create a 3D model of material layers. 3D printing technology today encompasses a wide variety of materials and methods. The structure and functions of the filaments used have become highly specialized, reaching the point where they can be used in the production of prosthetics and orthotics. In 3D printing, different organs and systems can be produced with different printing materials (18). CT and MRI scans can be used to create digital input for 3D printers in the form of stereolithography (STL) files. STL files can be modified with computer programs before printing, allowing you to make changes to the model (19).

1. Studies on Osteology

Bones, the basic building blocks of osteology, come together in a certain order to form the skeleton (20). Anatomical formations of bones can be examined through 3D models. Sex distinction can be made in animals by looking at their bones, and morphometric, volumetric and geometric measurements can be made on 3D models created from bones (21-30).

In a study conducted with rats, 3D modeling of the ossa membri thoracici was performed. Advanced processus (proc.) coracoideus and fossa subscapularis, and proc. hamatus and proc. suprahamatus structures were observed in the acromion. Margo cranialis is shorter than margo caudalis and the incisura scapulae is seen as a wide notch. Foramen (for.) supratrochleare and for. supracondylare were not observed in the humerus. It was observed that the radius and ulna were two separate bones; the tuber olecrani had three protrusions and a groove extending distally from the incisura trochlearis on the ulna. The length and width of the scapula and the latero-medial diameter measurements of the radius showed statistically significant differences between the genders, while no differences were observed in the humerus and ulna bones (21). There are many studies on Van cats. In one study, the clavicle and scapula bones were reconstructed. It was observed that the clavicle is located in front of the proximal end of the humerus and is a slightly curved bone independent of the other bones. While morphological differences were observed between the sexes in the clavicle and scapula bones, it was determined that the values were larger in men in volumetric measurements. Reconstructed images of the scapula are given in Figure 1 (23). In another study, humerus and antebrachium bones were reconstructed, morphometric and volumetric measurements were made, and differences between the sexes were evaluated. In general, it was observed that the measurement values were larger in male cats (24). A study in New Zealand rabbits used 3D reconstruction of various limb bones. As a result of examining the models, it was determined that the longest bone was the tibia. It has been stated that the parameters of the scapula, humerus, antebrachium, and tibia bones differ between the sexes and can be used for discrimination (28). In another study conducted with New Zealand rabbits, the humerus and femur, which are long bones, were examined. In male rabbits, it was observed that the bones on the right side had a larger volume and surface area than those on the left side. However, these differences were not considered significant in terms of gender discrimination and it was stated that the distinction could not be made here (31).

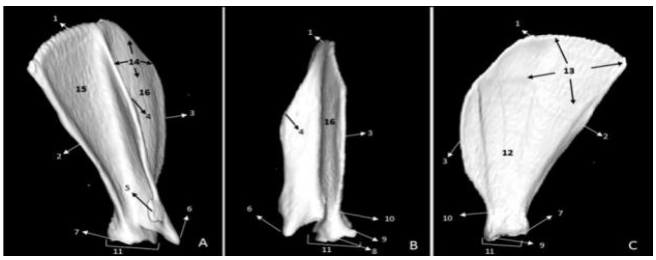

Figure 1. Reconstructed image of the scapula in the Van cat. **A:** Lateral view**, B:** Cranial view, **C:** Medial view (22).

In a study, the bones of the ossa membri thoracici and ossa membri pelvin of the gazelle (*Gazella subgutturasal*) species were examined. It has been stated that the longest bone is the tibia, and when the overall skeletal system is examined, differences are seen between the sexes and can be used for distinction (22). In a study conducted with Van cats, 3D reconstruction of ossa carpi, ossa metacarpalia I-V and ossa digitorum manus bones was performed. When morphometric and volumetric measurements were examined, it was determined that the differences between male and female cats were significant and the values were higher in male animals (25). In another study conducted with Van cats, 3D reconstruction of the metatarsus and phalanx bones was performed. According to the measurement results obtained, most measurement values in male animals were found to be higher than in female animals. In addition, the length order of the metatarsus bones was determined as IV, III, V and II (26). In a study conducted with Siirt colored angora goats, 3D reconstruction of the bones forming the os metacarpus and ossa digitorum manus (phalanx proximalis, phalanx media and phalanx distalis) was performed. Values differing between genders were measured higher in male animals (29). In a study conducted on the brown bear (*Ursus arctos*), the ossa cruris was examined using MDCT. It has been observed that the tibia and fibula bones articulate and unite in the proximal and distal parts (32).

In a study conducted with Van cats, morphometric values of the cranial and caudal diameters transversa of the cavum pelvis were determined from reconstructed models and gender differences between these indicators were examined. A relationship was observed between age and the cranial and caudal opening of the cavum pelvis in female cats. In male cats, a significant relationship was observed between age and weight and dorsal, medial and caudal diameters transversa. Medial and caudal diameters transverse were measured larger in male cats. In addition, the inclination of the pelvis and the ischial arch were larger in female cats. It was also observed that the caudal aperture was larger than the cranial (33). In Kangal dogs, the diameter conjugata, diameter transversa and diamater verticalis of the cavum pelvis were examined and the angles in the pelvis were measured. It was observed that the diameters in the pelvic cavity were larger in males than in females (34).

In one study, 3D bone models were created from digital images of the dog cranium obtained via CT and 3D printing was done. The digital image and print model of the cranium are given in Figure 2 (35). In a study conducted with porcupine (*Hystrix cristata*), 3D modeling of the cranium was performed and then morphometric measurements and differences between the sexes were examined. As a result of the study, it was determined that the cranium length was the longest measurement, the shortest measurement was the palatal width; in the mandible, the longest measurement was the total mandible length and the shortest measurement was the margo interalveolaris (27). In a study conducted with Akkaraman and Kangal Akkaraman sheep breeds, after taking CT scans of the craniums of these animals, 3D models were created from these images and morphometric measurements were taken from them. As a result of the study, a significant difference was found in the parameters of cranium length and width, nasal length and width, cranial length and width, facial width, for. magnum height and width, os frontale width and short distance between two orbits as a result of statistical analysis. According to the results of geometric morphometric analysis, in the craniums of Akkaraman and Kangal Akkaraman breed male sheep; in the dorsal direction, there were differences in the protuberantia occipitalis externa, the junction of the coronal suture-interfrontal suture, the internasal suture and the anterior edge of the internasal fissure; and in the lateral direction, there were differences in the anterior end of the septalis process and the slope of the dorsum nasi towards the labium (36). In one study, 3D images were created from the cranium of seagulls to compare them with other birds. It has been stated that measurements taken from the cranium will help determine the taxonomic location of the seagull head (37). In a study, 3D reconstruction method was used to define the bone structures in the cranium of the capybara (*Hydrochoerus hydrochaeris*) rodent. It has been stated that bones can be selected thanks to these 3D models (38).

The jawbone (os mandible) of Romanov (*Ovis aries*) sheep breed was examined and its morphological features were determined. Differences between genders were evaluated in line with the obtained data. As a result of the measurements, it was determined that the volume and surface areas of rams were higher than those of females (30). In a study, 3D modeling of the os hyoideum bone of different animal species such as equide, ruminant, carnivorous, and sus was carried out. After scanning the os hyoideum bones, 3D modeling was done and 3D prints were produced from these models (39).

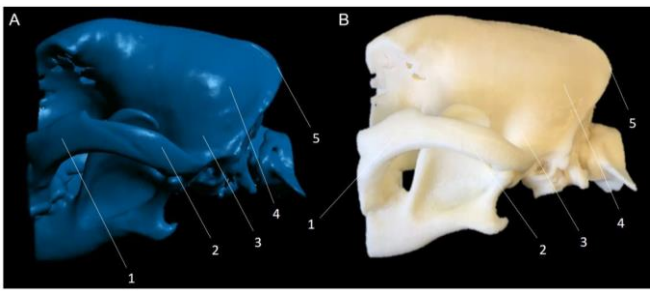

Figure 2. Digital and 3D printed model of the carnivore cranium. A, lateral view of digitized cranium bones. B, is the lateral view of the 3D printed biomodel. Proc. frontalis of os zygomaticus (1), proc. zygomaticus of os temporale (2), Os temporale (3), Os parietale (4), Os interparietale (5) (34).

In a study, in order to examine the detailed anatomy of the cervical joint surfaces (APJ) of horses and to look at its effect on the medulla spinalis, the 3D anatomy of the APJ in relation to the medulla spinalis was examined. As a result of the study, it was stated that APJ alone will not put pressure on the medulla spinalis and will not cause disease as long as

there is no soft tissue or bone damage in the region (40). In a study conducted with foxes (*Vulpes vulpes*), vertebrae cervicales were examined. The images were reconstructed in 3D and the vertebrae were compared by looking at the length and diameter of the corpus vertebrae of each vertebra except the first vertebra, and the diameter of the for. vertebrale. The average of each measurement value was calculated. Corpus vertebra length decreased from C2 to C7. The transverse diameter decreased from C2 to C4 and increased from C5 to C7. The sagittal diameter increased from C2 to C4 and decreased from C5 to C7. It was observed that the transversal and sagittal diameters of the for. vertebrae increased from C5 to C7 (40). 3D images of the columna vertebralis were examined using MDCT data in gazelles. The number of vertebrae was found to be 7 cervical, 13 thoracal, 6 lumbar, 5 sacral and 12-16 caudal (22).

2.Studies Related to Arthrology

Arthrology studies the relationships between the bones that make up the skeleton. The attachment of these structures to each other is in the form of synarthrosis (immobile), diarthrosis (mobile) and amphiarthrosis (semi-mobile). Joints enable movements such as abduction, adduction and rotation (20,42). Since these movements are more important in some breeds, the structures that form them have been examined (43,44). Diseases such as hip dislocations is important disorders related to the movement mechanism (45).

In a study conducted with French Bulldogs, since the femoral external rotation and abduction angle are higher than other breeds, the effects of the movements in the leg on the patella were examined using 3D images. It was concluded that diagnosis and treatment can be applied more easily by looking at these images (44). In this study, the accuracy of a 3D automated method (computer-aided design, aCAD) used to measure three different femoral angles in dogs: anatomical lateral distal femoral angle (aLDFA), femoral neck angle (FNA), and femoral torsion angle was evaluated. It has been stated that the obtained 3D models have a high accuracy rate, therefore the method can be used in patella luxation, femoral degenerations and in the design of patient-specific hip prosthesis structures. It has been said that the most important advantage of this method is that it eliminates user-induced measurement differences by automatically calculating femoral angles (43).

The structure of the art. genus was examined by performing 3D reconstruction using MRI and MDCT in New Zealand rabbits. When statistical measurements were examined, differences were observed in rabbits of the same weight and different genders. The image of art. genus is given in Figure 3 (46). In a study, 3D reconstruction of the lig. sacrotuberale, which is important for hip dislocations and perineal hernias in dogs, was performed. As a result of dissection and morphometric measurements, no statistical difference was found between the right and left lig. sacrotuberale (45). In a study, 3D evaluation of the art. glenohumeralis was performed in sheep, cats, and rabbits. When the results were examined, it was found that the highest values were generally in sheep and the lowest values were in cats (47).

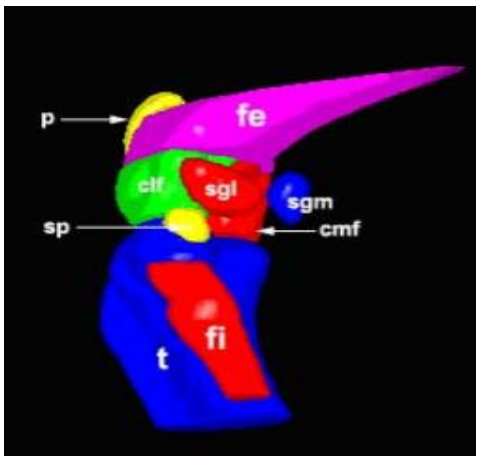

Figure 3. Lateral view of the left side art. genus of the New Zealand rabbit (45).

3. Studies on the Systema Digestorium (Digestive System)

The digestive system is important for the nutrition and development of the animal. In order to correctly diagnose disorders that may occur in the organs of this system and to perform appropriate interventions, the relevant organs must be well known. Practical training can be done on these organs by taking print models (48). Digestive system organs may differ among animal species (20,42). It is difficult to access cadavers of every animal species or to ensure the preservation of these organs. The similarity of 3D printing models with real organs and the use of these models in education have been evaluated (49-51).

In a thesis study conducted with New Zealand rabbits, the gastro-intestinal system (GIS) organs of these animals were examined. As a result of measurements made on 3D models, the ratios of the surface areas of the gaster, caecum, and intestines other than caecum to the total digestive system surface area were determined as 11%, 39%, and 48%, respectively. The ratios of the volumes of the same structures to the total system were calculated as 17% for the stomach, 59% for the caecum, and 23% for the intestines. As a result of length measurements performed on dissected animals, it was determined that the longest intestinal section was the jejunum (11). In one study, a 3D printing model of the upper digestive tract of dogs was created. Students stated that the model was useful and understandable. It was also stated that the model would be beneficial for endoscopy applications (48). In a study on the upper digestive system of rabbits (*Oryctolagus cuniculus*), the organs were visualized by X-ray. The philtrum structure, sulcus medianus lingua, and torus lingua structures were observed. Filiform papillae, fungiform papillae, foliatae papillae, and vallatae papillae were observed on the tongue (52).

When examining the teeth of horses, the aim was to observe changes in the distance (dentin thickness) between the cavum pulpa and the facies occlusalis and labialis of the incisors over time. The examinations revealed that the dentin thickness between the cavum pulpa and the facies occlusalis decreased with age in the upper and lower incisors, while the thickness between the cavum pulpa and the facies labialis increased (53). The dental anatomy of the Narwhal (*Monodon monoceros*) was studied using CT and 3D software. The positions of the remaining teeth in the jaw were examined (54). Another study aimed to create 3D anatomical models of the lingua of domestic mammals (cows,

dogs, horses, and pigs). Anatomical features and species-based differences in lingua print patterns were easily identified (49).

In a study, the anatomical structure of the sheep gaster was examined through 3D modeling and printing. It was scaled down and printed, taking into account its anatomical structure. It has been stated that these models are very similar to the real ones in terms of morphology and appearance and will be useful as educational materials. The image of gaster is given in Figure 4 (50). In a study conducted with sheep gaster, 3D printing models were created using the fusion deposition modeling (FDM) method. In the survey conducted among first-year veterinary faculty students regarding whether there is a difference between real gaster and 3D printed models and the ability to select anatomical structures in printed models, no morphological difference was reported and equal identification was possible (50).

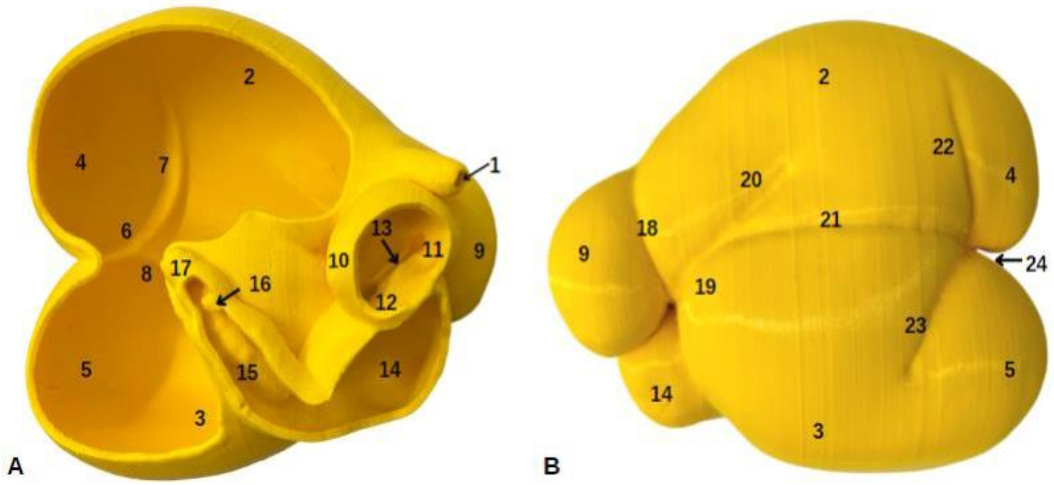

Figure 4. Small ruminant open gaster model. Views from right (A) and left (B). Esophagus (1); saccus dorsalis (2) and saccus ventralis (3); saccus caecus caudodorsalis (4) and saccus caecus caudoventralis (5); pila caudalis (6); sulcus coronarius dorsalis (7) and sulcus coronarius ventralis (8); reticulum (9); omasum (10); ostium reticulo-omasicum(11); ostium omaso-abomasicum (12); sulcus omaso-abomasicum (13); abomasum (14); pars pylorica of the abomasum (15); torus pyloricus (16); duodenum (17); sulcus ruminoreticularis (18); sulcus cranialis (19); sulcus accessorius sinister (20) and sulcus longitudinalis sinister (21); sulcus coronarius dorsalis (22) and sulcus coronarius ventralis (23); sulcus caudalis(24) (50).

In a study on cat hepar, the branching of the arterial, venous, and biliary tracts of 6 cat cadavers were examined in 3D. Their computerized tomography angiography (CTA), 3D printing and epoxy injected forms were examined and they were examined among themselves. As a result of the examinations, the arterial, venous, and biliary pathways associated with each lobus hepatis could be identified with the help of 3D prints. It has been stated that the cat hepatic system is different from that of dogs. Images of these are given in Figures 31 and 32 (55).

4.Studies on Systema Respiratorium (Respiratory System)

Respiration is a system consisting of the basic organs that provide gas exchange between the atmosphere and the blood of the living being and the auxiliary organs responsible for the transmission of this air (20). When looking at the cranium, the cavum nasi and the paranasales sinus are the most complex structures in terms of the respiratory system. These structures need to be known for correct diagnosis and treatment in case of any disease that occurs in the region (56-59).

In a study conducted with zebu cattle (*Bos Taurus Indicus*), the cranium was examined. Four nasal conchae (named dorsal, medial, ethmoidalis, and ventral) and five paranasal sinuses (sinus frontalis, maxillaris, palatinorum, and lacrimalis) were identified on CT image. Sinus frontalis was found to be the most complex sinus (59). In a study conducted with male Tuj sheep, cavum nasi and paranasales sinuses were examined. It has been stated that the sinus frontalis has the largest volume and the sinus lacrimalis has the smallest volume (56). In a study, 3D reconstruction of the paranasal sinuses in ponies was performed and examined. In the examinations, it was seen that the paranasal sinus consists of 7 sinuses, as in large horses. It has been observed that sinus volume increases in proportion to cranium length in animals younger than 6 years of age (58). In a study conducted with Holstein cattle, CT scans were performed after examining the cross-sectional anatomy of the cavum nasi and paranasales sinuses, and then 3D reconstruction was performed. The visual of these structures is given in Figure 5. In 3D models, the structures in the cavum nasi and paranasalis sinuses could be easily selected. As a result of the evaluations, it was found that the sinus sphenoidalis was the smallest and most asymmetric sinus, while the sinus frontalis was the sinus with the most complex structure, surrounding almost all the bones around the cavum cranii. It has also been stated that the ethmoidale is the only bone directly related to all airways (except for the sinus and cellulae of the concha nasalis ventralis). As a result of morphometric measurements, it was determined that there was no significant difference between the right and left sides (57).

In a study conducted with Kangal dogs, a 3D examination of the trachea, one of the respiratory system organs, was made. When looking at the models, it was stated that the trachea was dorsoventrally flattened and partially ellipsoid-shaped (60). In a study on the respiratory system organs of the Egyptian tortoise (*Testudo kleinmanni*), 3D examination of the organs was performed using a digital camera and CT. As a result of the study, it was seen that the trachea was

shorter compared to other animal species, and the other structures were generally compatible. Initially, the pulmonary arteries had a homogeneous appearance, but they later became divided into regions with no respiratory function. This change is said to increase the curvature of the upper shell, enabling the turtle to easily right itself after falling on its back (61). In a study conducted with New Zealand rabbits, CT scans of the respiratory system organs were taken and then, using 3D images and biometric values, the volume and surface area of these organs were calculated as 68028 mm^3 and 22447 mm^2, respectively (62).

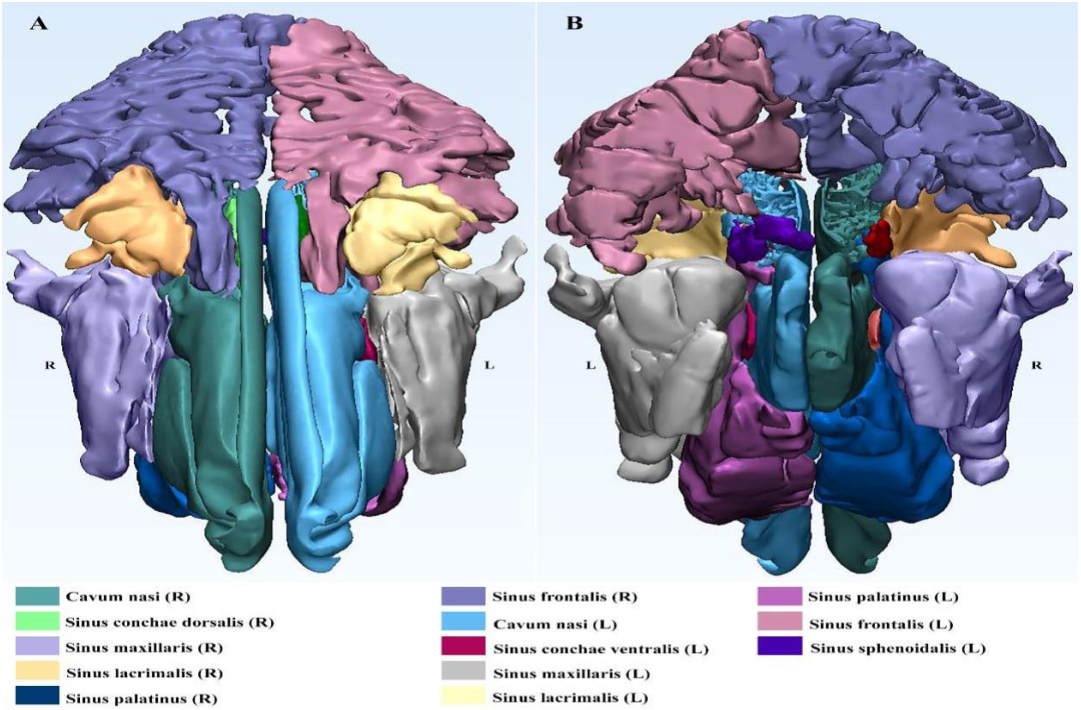

Figure 5. 3D reconstructed models of the cavum nasi and paranasales sinuses in holstein cattle. A (View from rostral), B (View from caudal) (56).

5.Studies on Systema Urogenitale (Excretory and Reproductive Organs)

Excretory and reproductive organs are structures located side by side and are important for the continuity of the living being and ensuring internal balance (20). These organs and their disorders can be examined using 3D modeling (63-66).

5.1. Organa urinaria (excretory organs)

In a study conducted on Kangal dogs, the anatomy of ren dexter and ren sinister was examined in 3D. The measurement value of ren dexter was found to be greater than that of ren sinister, and a rotation anomaly was detected in one of the ren dexters. Ren dexter and ren sinister are shown in Figure 6 (64). In another study conducted on New Zealand rabbits, 3D reconstruction of the rabbits using MDCT was performed to examine their biometric features. In the study, it was determined that ren dexter was larger than ren sinister in terms of volume and length and width. In addition, ren sinister was observed to be flatter than ren dexter (63).

In one study, the application of the retrograde CT urethra imaging technique in healthy female Beagle dogs was examined. It has been stated that the volume and diameter of the urethra may vary depending on whether the vesica urinaria is empty or full (66).

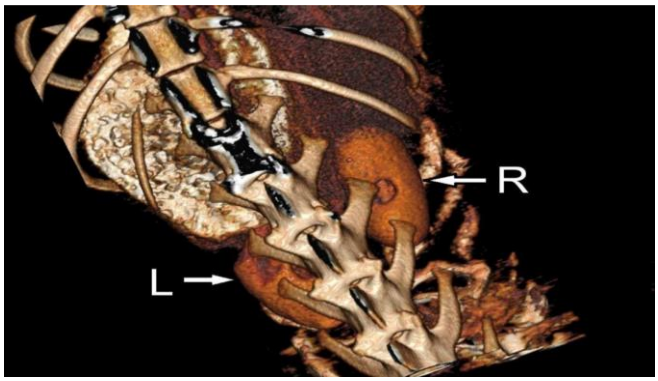

Figure 6. 3D view of Kangal dog ren. Dorsal plane, 3D view of ren dexter (R) and ren sinister (L) (63).

5.2. Organa genitalia (genital organs)

In a study on the male Red fox (*Vulpes Vulpes*), the organ genitalia was examined macroanatomically and 3D reconstructed. Anatomical findings showed that the testicle was oval-shaped and located horizontally in the scrotum. It is stated that only the prostate gland is located as glandulae (gl.) genitales accessoria and is positioned around the urethra. Os penis was observed within the pars spongiosa penis. No difference was found between the measurements taken from the digital caliper and the 3D model (65). In a study, the macroscopic and morphometric features of the os penis (baculum) of the brown bear (*Urcus artos*) were examined with the help of CT and digital caliper. A distinct sulcus urethralis

was detected on the bone, and it was determined that the measurements made with calipers and the data obtained from CT images were compatible with each other (66). In a study conducted with New Zealand rabbits, male reproductive organs were examined and some organs were evaluated with MRI. It has been determined that the prostate gland consists of three parts: proprostate, corpus prostate, and paraprostate, and the bulbourethral gland is the size of a green lentil and is found in pairs (68).

6.Studies on Systema Vasorum (Circulatory System)

Circulation, which has a specific network and routing structure throughout the animal's body, is a system that needs to be understood (42). The vascular structure and its distribution in the body have a complex structure. When surgical interventions are performed for disorders that occur, it is desired not to damage the structures in the region (69). The nutrition of organs depends on the condition of the vascular structures. Accurate knowledge of vascular structures is important in detecting any anomalies that may occur. Correct evaluation of the anatomical structure of the vessels may allow for more accurate diagnosis of diseases (70,71).

In one study, a 3D printing model of a dog's cor was created and its effect on student work was examined. In this study, two groups were formed to examine the video guide for anatomy with 3D printed models or using the video guide only. When the results were examined, it was observed that these models increased the impact of students on the course (72). Macroscopic sections and 3D reconstruction images of the cor of the dromedary camel were compared. When macroscopic sections and CT images were examined, more information about ventricular mass measurements was obtained (73).

In a study conducted on cranial vessels in pigs, the corrosion cast technique was applied to the arteries and then 3D reconstruction was performed on these models using cone beam computed tomography (CBCT). It has been stated that anatomical structures can be clearly seen in 3D models in accordance with reality. Images of these structures are given in Figure 7 (74).

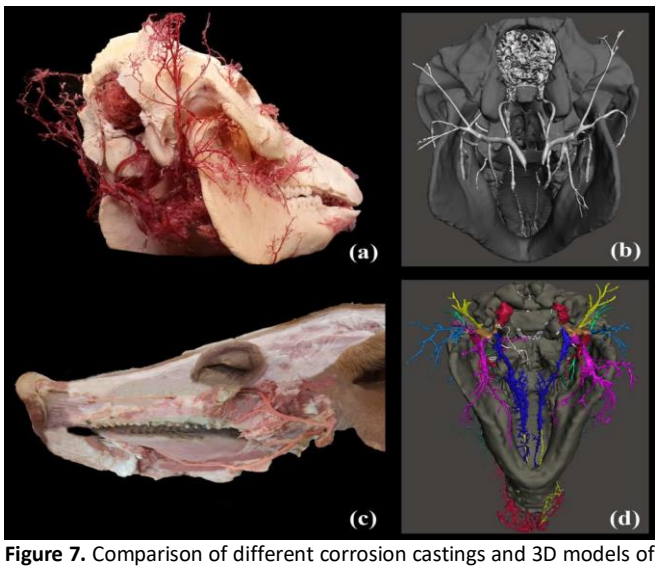

Figure 7. Comparison of different corrosion castings and 3D models of the sus cranium. (a) Laterocaudal view of duracryl plus corrosion casting sample, (b) caudoventral view of 3D model of duracryl plus corrosion casting sample, (c) lateral view of gelatin corrosion casting sample after partial dissection, and (d) ventral view of 3D model of gelatin corrosion casting sample (73).

In one study, abdominal vascularization of adult cats was examined using anatomical and diagnostic imaging techniques. As a result of the study, it was stated that normal vascular structures can be used as 3D models in veterinary clinics and may contribute to 3D modeling studies on vascular anomalies in the future (70). In a study, transcaval ureter anomaly was first described in dogs and cats and examined with CT. In the CT images, segmental duplication of the caudal venae cava in the prerenal segment and the formation of a vascular loop through which the ureter passes were seen in 3 cats and 2 dogs. In the images, this situation is described as a "double-barreled shotgun". The malformation is divided into two groups according to the arrangement of the branches of the caudal venae cava and their relationship with the aorta: Type I (symmetric, on the right lateral side of the aorta) and Type II (asymmetric, on the right dorsal side of the aorta). This anomaly was associated with hydroureter and mild pyelectasis in one case, while it was detected incidentally in three cases and its clinical significance remained unclear in two cases. CT has been evaluated as a suitable method in the diagnosis of this disease, but it has been stated that this congestive condition requires further clinical investigation (71).

In one study, the normal anatomy of the vessels in the abdomen and pelvis of two adult female cats was examined using contrast-enhanced CT angiography, non-contrast MR angiography, and 3D printing techniques. CT angiography demonstrated the major vessels in detail. In the images taken from MRI, the vessels were seen and selected brighter than the surrounding organs. It has been stated that the printed models show the main veins in terms of location and shape. It was stated that these images and models will contribute to future research (75).

7.Studies on Systema Nervosum (Nervous System)

The nervous system is a system that enables the interaction of the living being with its environment and keeps the body in a certain balance by working together with the immune system, endocrine and sensory organs (9). Disorders occurring in the ventricular system in the brain cause the formation of some diseases (76). Some anatomical structures in the brain play an important role in the diagnosis of an important zoonotic disease such as rabies (42,77). There are difficulties in identifying macroscopic structures and associating them with diseases (78,79).

In one study, 3D models were created from histological sections of the cervical region of the medulla spinalis of a thoroughbred English horse (80). In a study, the cerebrum structure of Akkaraman sheep was examined anatomically using the 3 Tesla MRI technique. As a result of morphometric measurements, it was determined that the cerebrum, hemispherium cerebri, cerebellum, and medulla oblongata structures were longer and wider in male animals. It has been observed that the left hemispherium cerebri is longer and the right hemispherium is higher in males; the left hemispherium cerebri is longer in females. As a result of volume measurements obtained from 3D reconstructed models, no significant difference was observed between genders (81). In a study, 3D sheep brain models were created using MRI scanning. It was stated that their printed models could be used for education (82). In a study on the ventricles

located in the encephalon in animals, 3D printing models of these were created. A survey was conducted among students to evaluate the effectiveness of the print models. According to the survey results, many students stated that the use of print materials was necessary and would facilitate the learning process. Ventricular system models are given in Figure 8 (83).

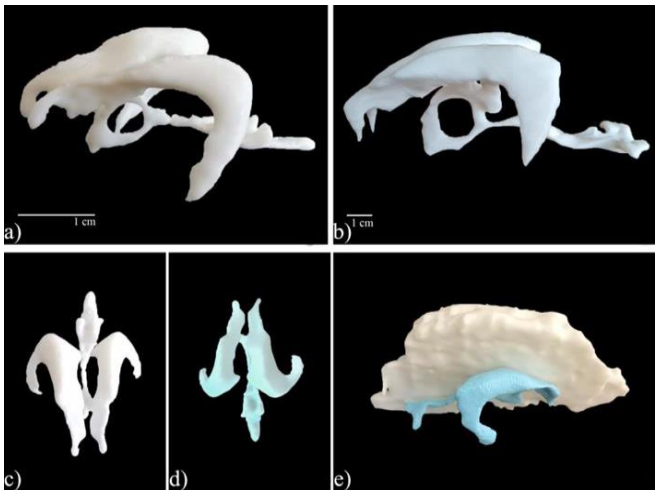

Figure 8. Different 3D printed ventricular system models in the dog. **a-** Normal 3D printed ventricular model of a dog, cranio-lateral view. **b-** Larger 3D printed ventricular model of a dog, lateral view. **c-**Normal 3D printed ventricular model of a dog, cranio-dorsal view. **d-** Normal 3D printed ventricular model of a dog, dorsal view. **e-** Normal 3D printed encephalon and entire ventricular system, cranio-lateral view. The right half of the encephalon was removed to show aspects of the entire ventricular system (82).

8. Studies on Organa Sensuum (Sensory Organs)

Organa sensuum includes the special and general senses that enable the living being to relate to its environment. It consists of the special senses of vision, hearing, balance, taste, and smell; and the general senses of touch, temperature, pain, and pressure. Sensory organs can be listed as organum olfactus (smell), organum gustus (taste), organum visus (eye), organum vestibulocochlearis (balance and hearing organ), and integumentum commune (touch) (42,84).

8.1.Organum vestibulocochleare (organ of balance and hearing)

Some anatomical structures are difficult to examine and use as educational materials due to their location and size. The structures within auris are also included in this group. Therefore, the evaluation of these structures using 3D models provides a more understandable and visually accessible approach (4,5,85,86).

In a study, computer-aided 3D models of the auris interna and auris media regions were examined in order to evaluate the effect of 3D models on anatomy education. In order to test the model in the study, one group was trained with models and the other group was trained with the traditional method. In the 15-question exam administered after the training process, it was determined that the first group (28 students) achieved an average of 83% success and the second group (29 students) achieved an average of 65% success (87). The auris interna of the rabbit was examined with 3D models. While the ossicula auditis was clearly observed macroscopically, it could not be observed clearly in CT images. It has been stated that in the images obtained from MRI, each of the fluids in the auris interna can not be clearly observed separately, but other structures can be seen easily. It was stated that labyrinthus osseus, labyrinthus membranaceus, and their subdivisions can be clearly seen and distinguished from each other in 3D models. Studies have shown that the structure of the auris interna of the rabbit is similar to human anatomy (86).

8.2. Organum visus (eye)

In an experimental study, retinal prostheses were intended to be made to restore vision to patients who had lost their visual functions. The organum visus of mouse, rat, and rabbit was examined anatomically and histologically. 3D images and models of these animals have been successfully generated, on which it was possible to identify the most suitable sites and ensure a safe implantation (88). In a study conducted with Brown Norway rats, 3D examination of the nervus opticus and the anatomical structures around it was performed and macroscopic and microscopic findings were examined. Some of their anatomical formations are given in Figure 9 (89). Micro-CT and macroscopic methods were used together for the volumetric evaluation of the bulbus oculi and its anatomical structures in Bama Miniature Sus, New Zealand rabbits, and Sprague-Dawley rats. For each organum visus, bulbus oculi, camera anterior bulbi, lens, and camera vitrae bulbi volumes were measured and imaged. The results showed that there are differences in the ratio of the anatomical structures of the organum visus to the volume of the bulbus oculi among different species. Especially in Sprague-Dawley rats, the ratio of the lens volume to the volume of the bulbus oculi was found to be the highest. This indicated that the possibility of damage to the lens during intra-ocular procedures may be higher. It was emphasized that the study could contribute to research in the field of ophthalmology (90).

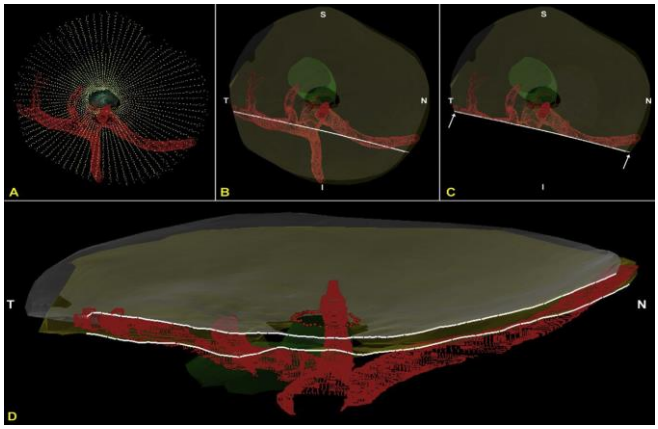

Figure 9. Anterior view of the arteria centralis retinae and surrounding arteries in the rat and the inner surface of the corpus vitreus (88).

8.3. Integumentum commune

In addition to being a sensory organ, the skin also has functions such as protecting the body, regulating temperature, and eliminating toxic substances. The integumentum communae is a comprehensive organ that includes structures such as subcutaneous connective tissue, dermis, epidermis, hair, nails, horns, mammary glands, and skin glands. The skin is a passive and active barrier that protects the body from the environment (9,20). Unlike other organs, 3D models of the skin have mostly been developed directly on humans

due to their architectural simplicity and easy accessibility. The development of these models appears to be beneficial in the fields of pharmacology, cosmetics, and the treatment of skin diseases (91).

9. Studies on Poultry

The systems and structures of poultry differ from those of domestic mammals. Some poultry species are economically important. The most prominent one is chicken, followed by goose, duck, and turkey (42). Due to their economic importance, the health of these animals is important and imaging techniques and 3D modeling are used for this purpose (92). Important structures include the flight mechanism (93,94) and the sacci pneumatici (95). In a study, MRI scans were performed on roosters and chickens and their 3D images were analyzed. It was stated that tissue differences and selections could be made in the reconstructed images, and the most appropriate sequences in MRI for poultry were determined (96). The use of micro-CT has become widespread in research on bone health. Micro-CT has been used in bone analysis in laying hens and has been reported to contribute to obtaining more information about their health status (92).

In a study on the European starling (*Sturnus vulgaris*), the muscles in the pectoral region were scanned with micro-CT and then 3D modeled. It was reported that the modeled muscles were accurate, but there were differences between the digital and real models. It has been stated that these differences are due to tissue complexity and data collection methods. However, it is said that modeling provides the opportunity to visualize all muscles in 3D and to make more accurate measurements (94). In a study with the falcon (*Accipiter nisus*), the muscles located on the cingulum membri thoracici were examined using contrast-enhanced micro-CT. Measurements were made and it was seen that the values obtained from these measurements were similar to the actual dimensions. Thanks to contrast micro-CT and 3D models, it was possible to evaluate the muscles in their real positions (93). A study was conducted on domestic ducks (*Anas domestica*) with three gl. linguales and a topographic study of the developmental stage and rate of these glands in relation to the os hyoideum bone. Rostral and caudolateral gl. linguales were located on the lateral parts of the cartilago entoglossum and os basibranchial, while caudomedial gl. linguales were located on the os basibranchial (97). Using imaging techniques, the 3D structures of the sacci pneumatici of birds were evaluated and models were created according to their sex and posture positions. Although the general anatomical structures of the sacci pneumatici were determined in the study using different poultry, they could not be analyzed in more detail. It was observed that there may be a difference in the volumes of sacci pneumatici in the relevant region, since the organa genitalia occupies a certain area in different sexes. It was stated that the study would be a basic source for sacci pneumatici and statistical analysis could not be performed due to the insufficient number of animals. Images of the sacci pneumatici in turkey (*Meleagris gallopava*) are given in Figure 10 (95).

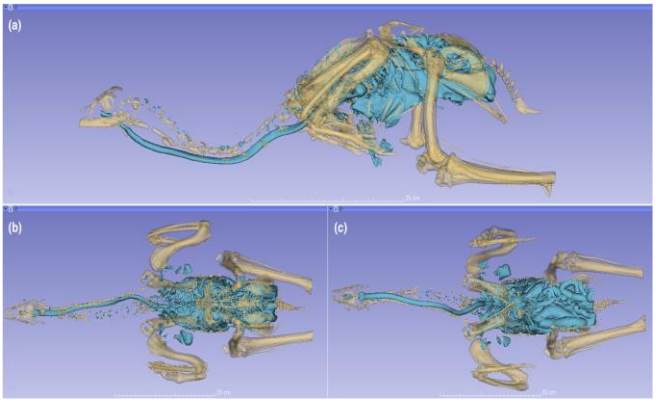

Figure 10. Sacci pneumatici in turkey (*Meleagris gallopava*). (a) Lateral view, (b) dorsal view, (c) ventral view (93).

CONCLUSION

When the contribution of anatomical reconstruction and 3D models to education is examined, it is seen that these methods are widely used in many structures and systems. Research shows that 3D models have positive effects on the learning process and yield successful results. Today, with technology becoming inevitable, 3D modeling stands out as an effective and efficient educational method. It is seen that this method provides a more hygienic and accessible learning environment and allows looking at structures that are difficult to reach. This increasingly widespread method makes important contributions to anatomy education. Looking at the studies we have compiled, we see that the most studies were conducted in the field of osteologia, followed by other systems. Although there are some deficiencies regarding the organs in these systems, it can be said that there are studies on each system in general. In the future, it is thought that these deficiencies will be closed and the contribution of 3D modeling to education will continue to increase with the additions to the existing information.

3D printing technology not only provides students with educational materials but is also very effective in maintaining the lives of sick animals. While simulated organs like prosthetic beaks, legs, ears, and other materials may not be as realistic, they do a great job of supporting and facilitating animal life. Therefore, it seems difficult to predict the future trajectory of 3D technology in veterinary anatomy.

ACKNOWLEDGMENT

We are grateful to the faculty members of the Department of Anatomy at the Faculty of Veterinary Medicine, Kafkas University, for their contributions to this review.

FINANCIAL SUPPORT

No financial support was received for the creation of this review.

CONFLICT OF INTEREST

The authors declare no conflicts of interest.

AUTHOR CONTRIBUTIONS

GKD: writing, reviewing, and editing; EK: writing and drafting; GKD-EK: writing and drafting.

REFERENCES

1. **Li F, Liu C, Song X, Huan Y, Gao S, Jiang Z (2018).** Production of accurate skeletal models of domestic animals using three-dimensional scanning and printing technology. *Anat Sci Educ.*, 11(1):73-80.
2. **Özkadif S (2015).** Some veterinary anatomical studies using three-dimensional reconstruction. *Batman Univ Yaşam Bilim Derg.,* 5(2):288-295.
3. **Singh N, Banga HS (2023).** Librarian-scientist (s) collaboration in harnessing the potential of augmented reality (AR) and virtual reality (VR) for veterinary and animal sciences education and training: A Success Story of Guru Angad Dev Veterinary and Animal Sciences University, Ludhiana, *I F L A.*
4. **Tan S, Hu A, Wilson T, Ladak H, Haase P, Fung K (2012).** Role of a computer-generated three-dimensional laryngeal model in anatomy teaching for advanced learners. *J LO.*, 126(4):395-401.
5. **Berney S, Bétrancourt M, Molinari G, Hoyek N (2015).** How spatial abilities and dynamic visualizations interplay when learning functional anatomy with 3D anatomical models. *Anat Sci Educ.*, 8(5):452-462.
6. **Elad D, Einav S (1990).** Three-dimensional measurement of biological surfaces. *ISPRS.*, 45(4):247-266.
7. **Mitchell HL (1995).** Applications of digital photogrammetry to medical investigations. *ISPRS.*, 50(3):27-36.
8. **Preece D, Williams SB, Lam R, Weller R (2013).** "Let's get physical": advantages of a physical model over 3D computer models and textbooks in learning imaging anatomy. *Anat Sci Educ.*, 6(4):216-224.
9. **Königh HE, Liebich HG (2022).** Domestic Animals Veterinary Anatomy Lecture and Color Atlas, 7. edition, Medipres publishing house, Ankara.
10. **Ohlerth S, Scharf G (2007).** Computed tomography in small animals–Basic principles and state of the art applications. *TVJ.*, 173(2):254-271.
11. **Dayan MO (2009).** Obtaining three-dimensional images from computed tomography images of the stomach and intestines in New Zealand rabbits. Doctoral thesis. Selcuk University Institute of Health Sciences, Konya., 30-45.
12. **Kaya T, Adapınar B, Özkan RAGIP (1997).** Basic Radiology Technique, 3.edition, Güneş & Nobel Bookstore, Bursa.
13. **Alkan Z (1999).** Computerized Tomography. Veterinary Radiology, Mina Ajans, Ankara.
14. **Girling SJ (2002).** Mammalian Imaging and Anatomy, *BSAVA* exotic pets handbook, 2.edition, Wiley Blackwell publication, Oxford, UK, 120-130.
15. **Memarian P, Pishavar E, Zanotti F et al. (2022).** Active materials for 3D printing in small animals: Current modalities and future directions for orthopedic applications. *Int J Mol Sci.*, 23(3):1045.
16. **Van Epps A, Huston D, Sherrill J, Alvar A, Bowen A (2015).** How 3D printers support teaching in engineering, technology and beyond. *Bulletin of the Association for Information Science and Technology*, 42(1):16-20.
17. **Anonymous:** https://www.ntboxmag.com/3d-yazicinin-mucidi-chuck-hull/ (Access: 21.04.2025).
18. **Vickram AS, Shofia S, Manikandan S et al. (2025).** 3D bio-printed scaffolds and smart implants: evaluating functional performance in animal surgery models. *Annals of Medicine & Surgery*, 87(6):3618-3634.
19. **Dickson J, Gardiner A, Rhind S (2022).** Veterinary anatomy education and spatial ability: where now and where next? *J Vet Med Educ.*, 49(3):297-305.
20. **Bahadir A, Yildiz H (2020).** Veterinary Anatomy Movement System & Internal Organs, 5.edition, Ezgi Bookstore, Bursa, 80-250.
21. **Kahraman S (2012).** Three-dimensional modeling of computed tomography images of ossa membri thoracici in rats. Master's Thesis. Selcuk University, Institute of Health Sciences, Konya.
22. **Demircioglu I, Gezer Ince N (2020).** Three-dimensional modelling of computed tomography images of limb bones in gazelles (*Gazella subgutturosa*). *Anat Histol Embryol.*, 49(6):695-707.
23. **Yılmaz O, Soygüder Z, Yavuz A (2020).** Three-dimensional investigation by computed tomography of the clavicle and scapula in Van cats. *Van Vet J.,* 31(1):34-41.
24. **Yılmaz O, Soygüder Z, Yavuz A (2020).** Anatomical, morphometric and volumetric examination of the humerus and antebrachium in Van cats by computerized tomography. *Harran Univ Vet Fac J.,* 9(2):161-169.
25. **Yılmaz O, Soygüder Z, Yavuz A (2020).** Three-dimensional examination of the skeleton manus in Van cats by computerized tomography. *Ataturk University J Vet Sci.,* 15(2):167-176.
26. **Yilmaz O, Koçyiğit A, Kırbaş Doğan G, Kanik B (2025).** Three-dimensional morphometric analysis of the metatarsal and phalangeal bones in Van cats. *Anat Histol Embryol.*, 54(1):e70006.
27. **Baygeldi SB, Güzel BC, Kanmaz YA, Yilmaz S (2022).** Evaluation of skull and mandible morphometric measurements and three-dimensional modelling of computed tomographic images of porcupine (*Hystrix cristata*). *Anat Histol Embryol.*, 51(4):549-556.
28. **Koçyiğit A (2023).** 3D Reconstruction of Some Extremity Bones in New Zealand Rabbits with 3D Scanner and Computerized Tomography. Doctoral Thesis. Selçuk University, Institute of Health Sciences, Konya.
29. **İşbilir F, Güzel BC (2023).** Investigation of metapodium and acropodium bones in Siirt-colored Mohair goat (*Capra hircus*) by 3D Modeling. *Harran Univ Vet Fac J.,* 12(2):245-252.
30. **İşbilir F, Güzel BC (2023).** Morphometric analysis of the mandible of ram and ewe Romanov sheep (*Ovis aries*) with 3D modelling: A CT study. *Anat Histol Embryol.*, 52(5):742-751.
31. **Selcuk ML (2023).** Computed tomography reconstruction and morphometric analysis of the humerus and femur in New Zealand rabbits, *Eurasian J Vet Sci.,* 39(4):164-170.
32. **Demircioğlu İ, Kırbaş Doğan G, Aksünger Karaavci F, Gürbüz İ, Demiraslan Y (2020**). Three-dimensional modelling and morphometric investigation of computed tomography images of Brown bear's (*Ursus arctos*) ossa cruris (Zeugopodium). *Folia Morphol.*, 79(4):811-816.
33. **Yilmaz O, Soyguder Z, Yavuz A, Dundar I (2020).** Three-dimensional computed tomographic examination of pelvic cavity in Van Cats and its morphometric investigation. *Anat Histol Embryol.*, 49(1):60-66.
34. **Atalar Ö, Koç M, Yüksel M, Arkaş AA (2017).** Three-dimensional evaluation of the pelvic cavity in Kangal dogs by computerized tomography. *F Ü Sağ Bil Vet Derg.,* 31:105-109.
35. **Bertti JVP, Silveira EE, Assis Neto ACD (2020).** Reconstrução e impressão 3D do neurocrânio de cão com o uso de tomografia computadorizada como ferramenta para auxiliar no ensino da anatomia veterinária. *Arq Bras Med Vet Zootec.*, 72:1653-1658.
36. **Baş Ekici H (2023).** Three-dimensional Modeling and Investigation of Morphometric Features of the Skull of Akkaraman and Kangal Akkaraman Sheep Using Computerized Tomography Images. Doctoral Thesis. Selçuk University Institute of Health Sciences, Konya, 30-55.
37. **İnce NG, Demircioğlu İ, Yılmaz B, Ağyar A, Dusak A (2018).** Three-dimensional modeling of the cranium in seagulls (*Laridae* spp.). *Harran Univ Vet Fac J.,* 7(1):98-101.
38. **Pereira F MAM, Bete SBDS, Inamassu LR, Mamprim MJ, Schimming BC (2020).** Anatomy of the skull in the capybara (*Hydrochoerus hydrochaeris*) using radiography and 3D computed tomography. *Anat Histol Embryol.*, 49(3):317-324.

39. **Bakıcı C, Akgün RO, Oto Ç (2019).** The applicability and efficiency of 3-dimensional printing models of hyoid bone in comparative veterinary anatomy education. *J A V M A.,* 90(2):71-75.
40. **Claridge HAH, Piercy RJ, Parry A, Weller R (2010).** The 3D anatomy of the cervical articular process joints in the horse and their topographical relationship to the spinal cord. *E V J.*, 42(8):726-731.
41. **Özkadif S, Halıgür A (2019).** Investigation of morphometric features of fox (*Vulpes vulpes*) cervical vertebrae using three-dimensional reconstruction. M A E Vet Fak Derg., 4(2):57-61.
42. **Dursun N (2007).** Anatomy of Domestic Birds, 4.edition, Medisan Publishing House, Ankara, 20-100.
43. **Longo F, Savio G, Contiero B et al. (2019).** Accuracy of an automated three-dimensional technique for the computation of femoral angles in dogs. *Vet Rec.*, 185(14):421-454.
44. **Lehmann SV, Andrada E, Taszus R, Koch D, Fischer MS (2021).** Three-dimensional motion of the patella in French bulldogs with and without medial patellar luxation. *BMC Vet Res.*, 17:1-12.
45. **Maviş CT, Selçuk ML (2022).** Morphometric and computed tomographic investigation of ligamentum sacrotuberale in dogs. *Vet Sci Pract.* 17(3):103-107.
46. **Sert ÖA (2009).** Obtaining three-dimensional data from dissection, computed tomography and magnetic resonance images of the knee joint in New Zealand rabbits. Doctoral thesis. Selçuk University, Institute of Health Sciences, Konya.
47. **Karabörk H (2009).** Three-dimensional measurements of glenohumeral joint surfaces in sheep, cat and rabbit by photogrammetry. *J A V A R.,* 8(7):1248-1251.
48. **Díaz-Regañón D, Mendaza-De Cal R, García-Sancho M et al. (2024).** Canine upper digestive tract 3d model: assessing its utility for anatomy and upper endoscopy learning. *Anim.*, 14(7):1070.
49. **Di-Donato BA, Dos-Santos AC, da Silveira EE et al. (2021).** Three-dimensional digitalized and printed tongue models of the cow, dog, pig and horse for undergraduate veterinary education. *Int J Morphol.*, 39(2):436-440.
50. **Mendaza-DeCal RM, Rojo C (2021).** 3D-printed model of the ovine stomach by surface scanning: evaluation for teaching veterinary anatomy, *Int J Morphol.*, 39(5):1480-1486.
51. **Torres MFP, Arce CP, Franco FM et al. (2024).** Production of 3D-printed ovine stomach models for animal anatomy education. *C L C S.,* 17(1):1339-1352.
52. **Kırbaş Doğan G, Duman Çabakçor E (2025).** A study on the morphometric, macroanatomical structure, and arterial vascularisation of the upper digestive system in rabbits (*Oryctolagus cuniculus,* Linnaeus 1758). *Vet Med Sci.*, 11(4):e70505.
53. **Englisch LM, Rott P, Lüpke M, Seifert H, Staszyk C (2018).** Anatomy of equine incisors: pulp horns and subocclusal dentine thickness. *E V J.*, 50(6):854-860.
54. **Tyler EM, Nweeia MT, Whitaker BR et al. (2008).** 3D Visualization of the Dental Anatomy of the Narwhal, Monodon monoceros. *J B C.*, 34(3):E44-E48.
55. **Rojo Ríos D, Ramírez Zarzosa G, Soler Laguía M et al. (2023).** Creation of three-dimensional anatomical vascular and biliary models for the study of the feline liver (*Felis* silvestris catus L.): A comparative CT, volume rendering (Vr), cast and 3D printing study. *Anim.*, 13(10):1573.
56. **Demiraslan Y, Dayan M, Ertılav K, Akbulut Y, Özkadif S, Özgel Ö (2020).** Computed Tomography Imaging of Cavum nasi and Sinus paranasales in the Tuj Sheep. *Dicle Univ Vet Fak Derg.,* 13(1):1-8.
57. **Turgut N (2021).** Cross-sectional radiological and 3D reconstructive anatomy of cavum nasi and paranasal sinuses in Holstein cattle. Doctoral Thesis. Selcuk University Institute of Health Sciences, Konya, 37-46.
58. **Köhler L, Schulz-Kornas E, Vervuert I et al. (2021).** Volumetric measurements of paranasal sinuses and examination of sinonasal communication in healthy Shetland ponies: Anatomical and morphometric characteristics using computed tomography. *BMC Vet Res.*, 17:1-8.
59. **Nomir AG, El Sharaby A, Hanafy BG, Abumandour MM (2024).** Head of Zebu cattle (*Bos Taurus indicus*): sectional anatomy and 3D computed tomography. *BMC Vet Res*., 20(1):318.
60. **Atalar Ö, Koç M, Özkan ZE, Baygeldi SB, Kanmaz YA (2018).** Three dimensional evaluation of trachea in Kangal dogs by computed tomography. *Harran Univ Vet Fac J.,* 7(2):133-137.
61. **Saber ASM, Kamal BM (2010).** Computed tomography and 3D reconstruction of the respiratory organs of the Egyptian tortoise (*Testudo kleinmanni*). *J Vet Anat.*, 3(1):1-15.
62. **Dayan MO, Besoluk K (2011).** Three-dimensional reconstruction from computed tomography images of respiratory system in New Zealand rabbits. *Eurasian J Vet Sci*, 27(3):145-148.
63. **Eken E, Çorumluoğlu Ö, Paksoy Y, Beşoluk K, Kalaycı İ (2009).** A study on evaluation of 3D virtual rabbit kidney models by multidetector computed tomography images. *Anat.*, 3(1):40-44.
64. **Atalar Ö, Koç M, Alklay AA, Arı HH (2017).** Three dimensional examination of kidneys in Kangal dogs by computed tomography. *Dicle Univ Vet Fak Derg.,* 10*(1)*:24-29.
65. **Halıgür A, Özkadif S (2019).** Male genital organs in the red fox (*Vulpes vulpes*); Macroanatomic and three-dimentional reconstruction aspect. *M A K U J Healt Sci Inst.*, 7(2):89-98.
66. **Kang K, Kim K, So J et al (2020).** The urethra of healthy female dogs can be normally narrowed due to the urethral flexure in retrograde CT urethrography. *Vet Radiol Ultrasoun.*, 62(1):61-67.
67. **Dalga S, Doğan GK, Akbulut Y, Çetin T, Kızılgöz V (2023).** CT imaging, macroanatomical and morphometric analysis of os penis in Brown bear (*Ursus arctos*). *Eurasian J Biol Chem Sci.*, 6(1):48-51.
68. **Bozbıyık C, Kırbaş Doğan G (2023).** Investigation of male genital system anatomy in the New Zealand rabbit (*Oryctolagus cuniculus* L.). *Anat Histol Embryol.*, 52(3):381-392.
69. **Oh M, Ban J, Lee Y et al. (2024).** Development of three-dimensional canine hepatic tumor model based on computed tomographic angiography for simulation of transarterial embolization. *Front Vet Sci.*, 10:1280028.
70. **Rojo D, Vázquez JM, Sánchez C et al. (2020).** Sectional anatomic and tomographic study of the feline abdominal cavity for obtaining a three-dimensional vascular model. *I J V R.*, 21(4):279.
71. **Spediacci C, Longo M, Specchi S et al. (2022).** Computed tomographic appearance of transcaval ureter in two dogs and three cats: A novel CVC congenital malformation. *Fron Vet Sci.*, 9:965185.
72. **Borgeat K, Shearn AI, Payne JR, Hezzell M, Biglino G (2022).** Three-dimensional printed models of the heart represent an opportunity for inclusive learning. *J V M E.*, 49(3):346-352.
73. **Alsafy MA, El-Gendy SA, Kamal BM et al. (2023).** Heart ventricles of the dromedary camel (*Camelus dromedarius*): new insights from sectional anatomy, 3D computed tomography, and morphometry. *BMC zool.*, 8(1):12.
74. **Tsandev N, Bakici C, Vodenicharov A (2022).** Evaluation of the compatibility between corrosion casts and 3D reconstruction of pig head arterial system on cone beam computed tomography. *Vet J Ankara Univ*., 69(4):419-424.

75. **Rojo Ríos D, Ramírez Zarzosa G, Soler Laguía M et al. (2023).** Anatomical and three-dimensional study of the female feline abdominal and pelvic vascular system using dissections, computed tomography angiography and magnetic resonance angiography. *Vet Sci.*, 10(12):704.
76. **Akdag R, Ozsoy U, Tüzün Y (2015).** Etiology and pathogenesis of hydrocephalus. *Turk Neurosurg.,* 5*(*1):15-18.
77. **Hazar S, Yarkın F, Akan E (2000).** Rabies and its importance. *Flora.,* 5(3):159-167.
78. **Schoenfeld-Tacher RM, Horn TJ, Scheviak TA, Royal KD, Hudson LC (2017).** Evaluation of 3D additively manufactured canine brain models for teaching veterinary neuroanatomy. *J V M E.*, 44(4):612-619.
79. **Blázquez-Llorca L, Morales de Paz L, Martín-Orti R et al. (2023).** The application of 3D anatomy for teaching veterinary clinical neurology. *Anim.*, 13(10):1601.
80. **Bolat D (2017).** Three-dimensional reconstruction of the spinal cord of thoroughbred. *Eurasian J Vet Sci.,* 33(2):127-129.
81. **Aydoğdu S (2021).** Three-dimensional reconstruction of 3 tesla magnetic resonance images of sheep brain. Doctoral Thesis. Selçuk University, Institute of Health Sciences, Konya.
82. **Haroglu D, İşcan B, Düzler A (2022).** Use of three dimensional (3D) printed models of sheep brain in online veterinary anatomy education. *Int J Print.*, 6(3):370-381.
83. **Ekim O, Bakici C, Akçay A, Algin O, Oto Ç (2024).** The efficiency of 3d-printed dog brain ventricular models from 3 tesla (3t) magnetic resonance ımaging (mrı) for neuroanatomy education. *Pak Vet J.*, 44(2):430-436.
84. **Yıldız D (2024).** Anatomy Mind Notes, 1.edition, *Güneş Medical Bookstores*, Ankara, 7-168.
85. **Balcombe J (2001).** Dissection: The scientific case for alternatives. *J A A W S.*, 4(2):117-126.
86. **Abd El-Hameed ZS, El-Shafey AAEF, Metwally MA, Abd El-Samie HAER, Kassab A (2023).** Anatomy of the rabbit inner ear using computed tomography and magnetic resonance imaging. *Anat Histol Embryol.*, 52(3):403-410.
87. **Nicholson DT, Chalk C, Funnell WRJ, Daniel SJ (2006).** Can virtual reality improve anatomy education? A randomised controlled study of a computer-generated three-dimensional anatomical ear model. *Med Educ.*, 40(11):1081-1087.
88. **Wang J, Walter P, Baumgarten S (2022).** Surgical anatomy of the small animal eye-3D reconstruction and ablation effect. *İ O V S.*, 63(7):4517-F0304.
89. **Pazos M, Yang H, Gardiner SK et al (2015).** Rat optic nerve head anatomy within 3D histomorphometric reconstructions of normal control eyes. *Exp Eye Res.*, 139:1-12.
90. **Wu Y, Feng Y, Yang J et al. (2024).** Anatomical and micro-CT measurement analysis of ocular volume and intraocular volume in adult Bama Miniature pigs, New Zealand rabbits, and Sprague-Dawley rats. *Plos.*, 19(9):e0310830.
91. **Fernandez-Carro E, Angenent M, Gracia-Cazaña T et al. (2022).** Modeling an optimal 3d skin-on-chip within microfluidic devices for pharmacological studies. *Pharm*, 14(7):1417.
92. **Chen C, Kim WK (2020).** The application of micro-CT in egg-laying hen bone analysis: introducing an automated bone separation algorithm. *Poult Sci.*, 99(11):5175-5183.
93. **Bribiesca-Contreras F, Sellers WI (2017).** Three-dimensional visualisation of the internal anatomy of the sparrowhawk (*Accipiter nisus*) forelimb using contrast-enhanced micro-computed tomography. *Peer J.*, 5:e3039.
94. **Sullivan SP, McGechie FR, Middleton KM, Holliday CM (2019).** 3D muscle architecture of the pectoral muscles of European Starling (*Sturnus vulgaris*). *İ O B.*, 1(1):oby010.
95. **Petnehazy O, Csoka A, Fajtai D, Echols S, Donko T (2024).** CT-based 3D reconstruction and basic anatomical analysis of the 3D anatomy of the air sac system in domestic birds. *Anat Histol Embryol.*, 53(2):e13022.
96. **Ekim O, Oto Ç, Algın O, Bakıcı C (2013).** High resolution 3D magnetic resonance imaging of the visceral organs in chicken (*Gallus domesticus*) by 3 tesla MR unit and 15-channel transmit coil. *Vet J Ankara Univ.,* 60(4):229-233.
97. **Skieresz-Szewczyk K, Cornillie P, Jackowiak H (2018).** The development of lingual glands in the domestic duck (*Anas platyrhynchos f. domestica*): 3D-reconstruction, LM, and SEM study. *J Morphol.*, 279(3):319-329.